

## Full Paper

# Solid-State Au/Hg Microelectrode for the Investigation of Fe and Mn Cycling in a Freshwater Wetland: Implications for Methane Production

Shufen Ma,<sup>a\*</sup> George W. Luther III,<sup>a\*</sup> Jason Keller,<sup>b</sup> Andrew S. Madison,<sup>a</sup> Edouard Metzger,<sup>a</sup> David Emerson,<sup>c</sup> J. Patrick Megonigal<sup>b</sup>

<sup>a</sup> College of Marine and Earth Studies, University of Delaware, Lewes, DE, USA

\*e-mails: sma@udel.edu; luther@udel.edu

<sup>b</sup> Smithsonian Environmental Research Center, Edgewater, MD, USA

<sup>c</sup> American Type Culture Collection, Manassas, VA, USA

Received: August 15, 2007

Accepted: October 5, 2007

## Abstract

The solid-state voltammetric gold-amalgam microelectrode was used to measure multiple redox species (O, S, Fe and Mn) in situ at (sub)millimeter vertical resolution to elucidate rhizosphere processes in Jug Bay wetlands. In vegetated soil, a classic diagenetic redox sequence without any dissolved sulfide was observed in summer. However, the rhizosphere can be quite variable which is due to the introduction of O<sub>2</sub> to the anoxic sediments by plants. In nonvegetated soil, the vertical concentration–depth profiles were relatively constant. The presence of Fe(II), Mn(II) and soluble Fe(III) in deeper sediments indicates the oxidation of Fe(II) as well as the nonreductive dissolution of Fe(III) and the reductive dissolution of Fe(III) and Mn(III, IV) solids. Mn(III, IV) and Fe(III) redox chemistry is important in organic matter mineralization mediated by bacteria and in suppressing methane formation. In addition, Mn(III, IV) also can oxidize Fe(II) to supply Fe(III) for bacterial Fe(III) reduction. Studying Fe and Mn cycling via voltammetric methods can give insights to methane production and loss as there is no methane sensor for sediment work at present.

**Keywords:** In situ voltammetry, Gold/Amalgam (Au/Hg) microelectrode, Iron and manganese redox, Methanogenesis, Wetlands

DOI: 10.1002/elan.200704048

*Dedicated to Professor Ernö Pretsch on the Occasion of His Retirement from ETH Zürich*

## 1. Introduction

The gold/amalgam (Au/Hg) voltammetric microelectrode was developed and used by Brendel and Luther in 1995 [1] for marine sediment work. Since then, this technology has been applied in a variety of natural environments to study biogeochemical processes in situ. The solid-state microelectrode holds several advantages over potentiometric and amperometric sensors as it can measure multiple species simultaneously in one voltammetric scan. In situ measurements can quantify five of the seven principal redox species involved in early diagenesis (O<sub>2</sub>, Mn<sup>2+</sup>, Fe<sup>2+</sup>, HS<sup>-</sup>, and I<sup>-</sup>) as well as detect FeS and Fe(III) complexes [2].

The solid-state Au/Hg microelectrode has been used to measure the distribution of these redox components in the water column of lakes, estuaries, inland bays, the Chesapeake Bay, the Black Sea as well as hydrothermal vents [3–11] and in the porewaters of marine and freshwater sediments at (sub)millimeter vertical resolution [4, 12, 13]. Voltammetry is a powerful technique because it provides chemical speciation data (e.g. oxidation state and different

elemental compounds/ions) as well as quantitative data at a precision of 2% or better on several chemical species. In this paper, we report using voltammetric microelectrodes to study Fe and Mn geochemistry in fresh water wetlands where plants and microorganisms interact to regulate methanogenesis which has global warming implications. Real time monitoring of Mn(II) and trace metals in lake waters [14] has been reported using a flow-through voltammetric cell. Tercier-Waeber et al. [15] also tested individually addressable Ir-based microsensor arrays in lab standard solutions to obtain trace metal concentrations with high spatial resolution. To date only the solid-state Au/Hg microelectrode has been applied to determine Fe(II) and Mn(II) in real time at (sub)millimeter vertical resolution in aqueous sediments.

Wetlands, which account for 33% of methane emissions worldwide, are dynamic environments due to photosynthesis and subsequent organic matter mineralization. During organic matter decomposition, the microbial communities use electron acceptors (i.e., oxygen, nitrate, Mn(III, IV) and Fe(III) hydroxides, sulfate, CO<sub>2</sub> and acetate) in a

diagenetic sequence to obtain the maximal energy yield for growth [16]. Solid phase metal oxide reduction depends on the availability of these resources in the sediments, which is not a problem in terrestrial and nearshore systems. As iron is the most abundant element in Earth's crust, iron reduction plays a critical role in organic matter mineralization. Since methanogenesis has a low energy yield, it is suppressed when competing against pathways using  $O_2$ ,  $NO_3^-$ , Fe(III) and  $SO_4^{2-}$  [17]. It has been shown that Fe(III) reduction can suppress sulfate reduction in salt marshes [18, 19], and methanogenesis in fresh water wetlands [20, 21]. There has not been a methane sensor available for sediment profiling [17]. Our solid-state Au/Hg microelectrode can serve as a possible proxy signaling methane processes by providing in situ Fe and Mn redox speciation data.

Wetland vegetation can have profound influences on anaerobic carbon metabolism because roots can release dissolved organic carbon and introduce  $O_2$  into the predominately anoxic sediments [18, 22]. As a result, the rhizosphere can be characterized as a microenvironment with high reaction rates and intense fluxes. Fe(II) produced from Fe(III) (oxyhydr)oxide reduction can then be reoxidized chemically or biologically to form an active Fe redox cycle. Therefore, Fe cycling can be a dominant process in anaerobic carbon metabolism and can suppress production of methane, a greenhouse gas more potent (about twenty three times) than  $CO_2$  [23].

Because sediment chemistry varies in space and time, the determination of chemical reactions at the microscale is very helpful for understanding interactions between plants, minerals and microorganisms. These processes allow us to

understand how small-scale mechanisms can lead to large-scale ecosystem responses. However, direct measurement of all redox species in heterogeneous sediments without introducing artifacts by traditional core sampling methods (cut into 0.5 cm or larger sections and then extracted for their interstitial waters) is not an easy task. The solid-state voltammetric microelectrode can be applied to probe these microenvironments and characterize their properties. The Au/Hg microelectrode can be deployed in situ to measure multiple chemical species simultaneously with low (0.2–3  $\mu M$ ) detection limits [1, 5] and without consumption of analytes. In summer 2006, a solid-state Au/Hg glass microelectrode was used to determine O, S, Fe and Mn redox species in situ to investigate Fe and Mn cycling in vegetated and nonvegetated soils in Jug Bay wetlands (Maryland, USA, Fig. 1). Our objective was to understand how plant activities regulate iron cycling and methanogenesis as more detailed information on Fe (and Mn) cycling will lead to better information on methane processes.

## 2. Experimental

### 2.1. Sites

The Jug Bay Wetlands Sanctuary (Fig. 1) is located on a tidal freshwater reach of the Patuxent River, Maryland, USA. This freshwater tidal marsh site has regular flooding and no evidence of bioturbation (animal reworking of the sediments). The site is at the end of a railroad bed where a boardwalk was placed. On the sides of the boardwalk are vegetated areas whereas under the boardwalk there is no vegetation. Measurements were conducted in vegetated areas at sites ER1, ER2 and ER3, and nonvegetated areas (under the boardwalk) near site ER1.

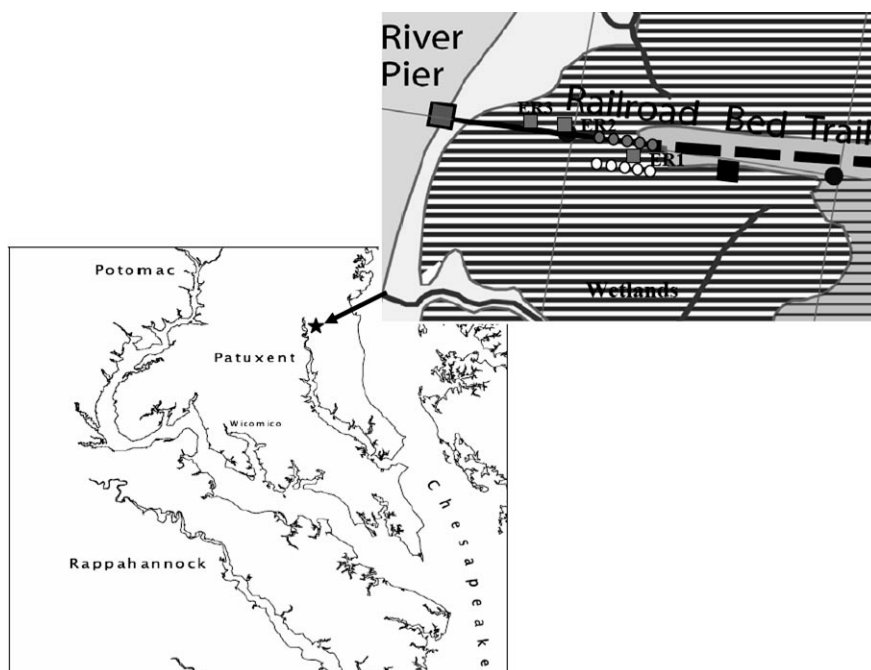


Fig. 1. Map of the Patuxent River. The star indicates the location of Jug Bay wetlands (38.78°N, 76.71°W). The insert shows the sampling sites which were at the end of a railroad bed where a boardwalk was placed. On the sides of the boardwalk are vegetated areas whereas under the boardwalk there is no vegetation. Measurements were conducted in vegetated areas at sites ER1, ER2 and ER3, and nonvegetated areas (under the boardwalk) near site ER1.

vegetated areas whereas under the boardwalk there is no vegetation. Sites are numbered from the end of the railroad bed to the river (ER1 through 3) that feeds the wetland. ER1 was dominated by *Typha latifolia* (cattail); ER2 was dominated by intermixture of *Typha latifolia* and *Peltandra virginica*; and ER3 was mainly *Nuphar advena*. Organic matter decomposition by sulfate reduction is not a significant process in this environment, but organic matter decomposition by manganese oxide and iron(oxyhydr)oxide reduction is significant.

## 2.2. Voltammetry

A solid state gold-amalgam (Au/Hg) glass microelectrode was used to measure dissolved  $O_2$ , Fe(II) and Mn(II) concentrations and to detect the presence of soluble Fe(III) and FeS molecular clusters in situ. The Au/Hg electrode was constructed from 100  $\mu\text{m}$  gold wire and encased in borosilicate glass with a total diameter of gold and glass near 200  $\mu\text{m}$ . The glass was drawn by a glass blower and was symmetrical around the long axis. A solid-state Ag/AgCl reference (500  $\mu\text{m}$  Ag wire) encased in glass with a vycor frit and a counter (Pt) electrode (500  $\mu\text{m}$  Pt wire) were used and constituted a three-electrode voltammetric system [1, 4, 5]. The solid state voltammetric electrodes were coupled with an Analytical Instrument Systems, Inc. model DLK-60 electrochemical analyzer and a laptop computer to perform real time voltammetry. Cyclic voltammetry (CV) was used for the in situ analysis. The voltage scan range was from  $-0.1$  to  $-1.8$  V. The scan rate was 2 V/s. A potential of  $-0.9$  V for 5 s was used as the conditioning step to maintain reproducibility. This first conditioning step removes any Mn(II), Fe(II), Fe(III) or S(-II) that may be present from the Au/Hg surface. A second conditioning step of 2 s was performed at the initial potential of the scan. A micromanipulator was used to hold the microelectrode for profiling sediments in the field. The glass electrode was pushed down with a vertical resolution from 0.1 mm to 1 cm until it met hard resistance.

The standardization and calibration of the electrodes have been documented in several papers and include the effects of pH and salinity [1], fluid flow rate and pressure [7] and temperature [2] on current. Waters from the site were collected to generate current versus concentration standard curves with standards for each chemical and were then used to calculate the in situ concentrations of  $H_2S$ , Fe(II), Mn(II) and  $O_2$ . Precision is typically better than 2% at the 95% confidence limit in lab experiments on the same sample. For our wetland work, 90% of the  $O_2$  and  $Fe^{2+}$  data and 80% of the  $Mn^{2+}$  data for at least three replicates at each depth are typically better than 5% RSD. We noticed larger variations when there were low concentrations or when the microelectrode passed into the roots. These standard deviations at each depth are significantly lower than the two to three orders of magnitude change in concentration observed over each profile. The detection limits for  $O_2$ , Fe(II) and Mn(II) are about 3  $\mu\text{M}$  and 0.2  $\mu\text{M}$  for  $H_2S$ . Standardizations of the

Au/Hg electrode were performed in the lab before field sampling and the electrode was rechecked after return to the laboratory. For peaks that are near in potential we used commercial software as in Brendel and Luther [1] or the voltammetry manufacturer's advanced analysis package (AIS) to discriminate and quantify peaks. Taking the derivative of the CV or LSV voltammograms also provides peak and baseline information for quantification.

## 2.3. Porewater $CH_4$ Determination

Five pairs of sippers, porewater suction devices [24] (Fig. 1), that ran parallel to the boardwalk were placed at a depth of 10 cm to collect porewater for methane measurements. One set of sippers (five white dots) was in vegetation ca. 10 ft from the boardwalk; the second set of sippers (five grey dots) was under the boardwalk. The ER1 site was roughly in the middle of the sipper line. After collection, porewater  $CH_4$  was measured by headspace equilibration-gas chromatography [21].

## 3. Results and Discussion

Iron and manganese geochemistry was investigated at (sub)millimeter scale to elucidate rhizosphere processes in summer 2006. Representative voltammograms from this freshwater site are shown in Figure 2 and show the transition of chemical speciation and changes in sediments. These were used to generate the concentration versus depth profiles in Figures 3 (vegetated sites) and 4 (nonvegetated sites).

Vertical profiles (Fig. 3a) were obtained in vegetated areas at site ER1 at the end of the railroad bed and beginning of the boardwalk. In situ determination indicates that  $O_2$  and Mn(II) were both present and overlap in the surface of the sediment.  $O_2$  was undetectable below 1.7 mm, whereas Mn(II) reached the highest concentration at 2.8 mm and was undetectable below 12 mm. Fe(II) and soluble Fe(III) were measured below 2.8 mm and increased at deeper depths. Fe(II) was over 2 mM below 10 mm. FeS was not detected. This diagenetic redox sequence of chemical species is as expected based on previous work [16, 25].

At site ER2 which is also a vegetated area, in situ measurements were conducted at two locations of 2 cm apart indicating that Mn was the dominant species at this site (Fig. 3b, 3c).  $O_2$  and Mn(II) were also found to overlap here. Figure 3b shows the fluctuation of  $O_2$  in shallow depths of sediments. At 2 cm away from the location of Figure 3b,  $O_2$  was measured from surface to 1.5 mm and at a few depths below 2 cm in the soil (Fig. 3c). The solid-state microelectrode detected the heterogeneity of the sediments caused by plants allowing  $O_2$  to pass into deeper sediments.

At site ER3 (Fig. 3d), which is another vegetated area closer to the river,  $O_2$  was only present in the upper 2.5 mm. Mn(II) and Fe(II) were detected in succession at deeper depths consistent with the diagenetic sequence expected

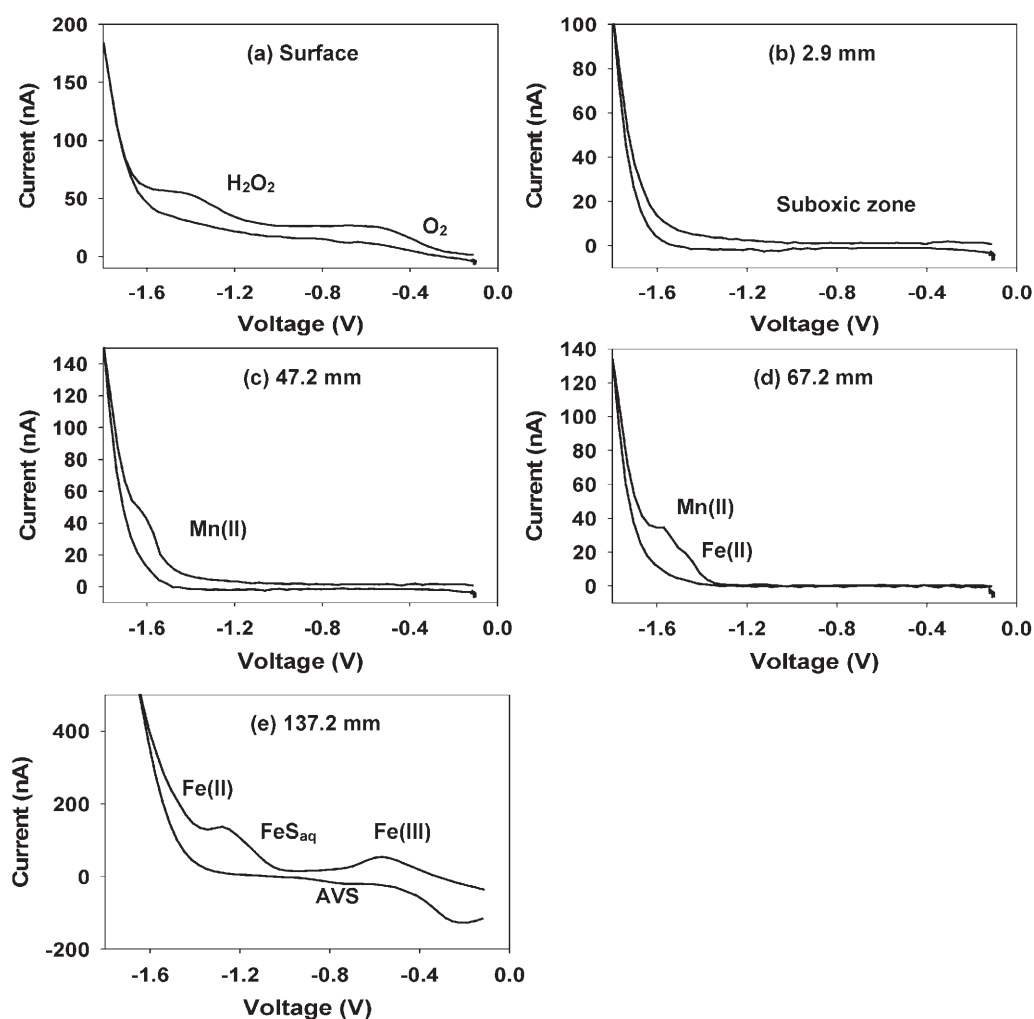


Fig. 2. Representative voltammograms collected at a range of depths in sediments at site ER3. Examples include oxygen (a), nondetectable levels of all redox species (b), Mn(II) (c), both Fe(II) and Mn(II) (d), and soluble Fe(III),  $\text{FeS}_{\text{aq}}$  and AVS (e).

[16, 25]. In addition, soluble Fe(III) and FeS were also found. FeS likely results from decomposition of organic matter that releases sulfide, which reacts with Fe(II), or minor amounts of sulfide from sulfate reduction. Soluble Fe(III), which is likely stabilized by plant exudates or chelates [26], forms from nonreductive dissolution of Fe(III) solids.

The profiles in nonvegetated areas (under the boardwalk near site ER1, Fig. 4a, b) contrasted strongly with the vegetated soils.  $\text{O}_2$  was undetectable, but Mn(II), Fe(II) and soluble Fe(III) were measured. At one location (Fig. 4a), Mn(II), Fe(II) and soluble Fe(III) had little change with depth. A signal for FeS was detected at depths below 1.4 mm. FeS corresponds to a cluster complex and has been observed in a variety of environments [27]. At 2 cm away from this location (Fig. 4b), Mn(II), Fe(II) and soluble Fe(III) were consistent at shallow depths; however, Fe(II) was much higher at deeper depths.

From June to August, porewater  $\text{CH}_4$  concentrations collected from a depth of 10 cm (Fig. 5) show a trend that dissolved  $\text{CH}_4$  at the vegetated site was lower than the

nonvegetated site. The biggest  $\text{CH}_4$  concentration difference (3.5 times) was observed in July. Our in situ profiling was conducted in August when porewater  $\text{CH}_4$  concentration in the nonvegetated site was still 1.4 times higher than at the vegetated site.

Although a classic diagenetic redox sequence without any dissolved sulfide was observed in summer, comparison of Figures 3a and 3d show that there is significant variability with depth and location. The rhizosphere can also be quite variable and plant roots (live and dead) can introduce  $\text{O}_2$  in significant quantities as in Figure 3c or in trace and nondetectable (Fig. 3b and 3d) amounts deeper into the sediments. The irregular profiles in Figure 3b and 3d indicate that there may be small amounts of  $\text{O}_2$  that enter the anoxic zones and then cause rapid Fe(II) and Mn(II) oxidation and/or that there is a change in sediment chemistry including the type of organic matter being decomposed and the use of metal oxides as electron acceptors. The presence of Fe(II), Mn(II) and soluble Fe(III) in deep sediments indicates the oxidation of Fe(II) as well as the reductive and nonreductive dissolution of Fe(III) and Mn(III, IV) solids. Voltammetric

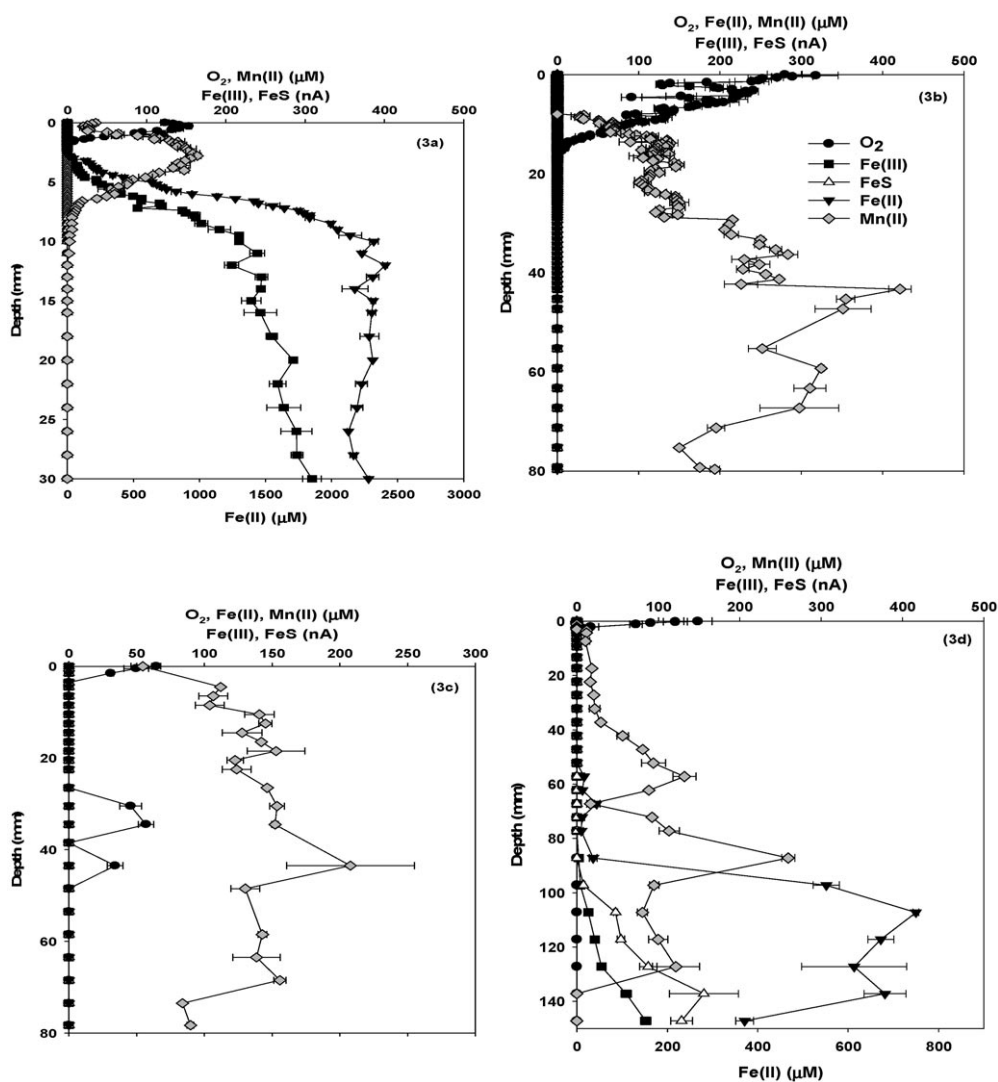


Fig. 3. Profiles from vegetated areas at a) ER1 (Aug. 8, 2006); b), c) ER2 (Aug. 9, 2006) at two locations of 2 cm apart, and d) ER3 (Aug. 9, 2006). Note that the symbols can be the same or smaller size of the error bars for 3–5 replicate scans.

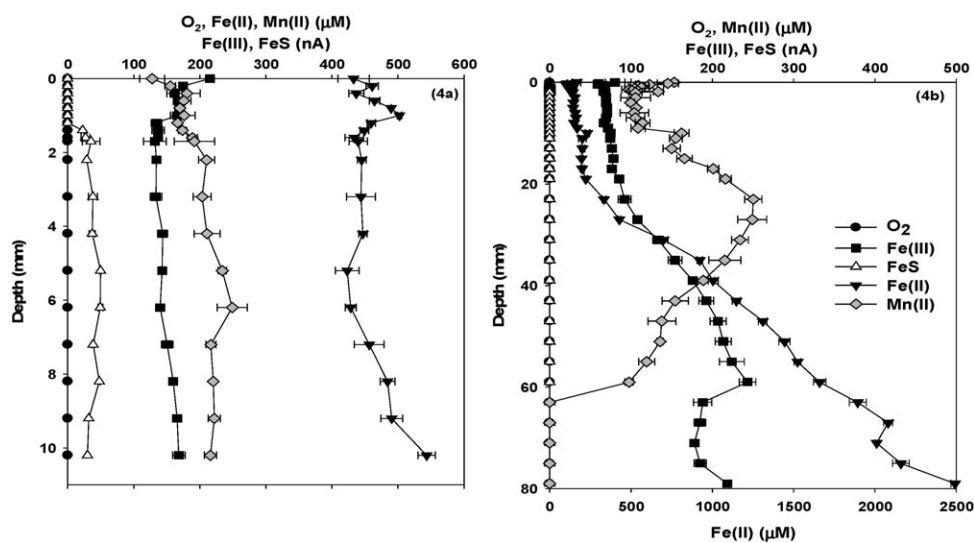


Fig. 4. Profiles from nonvegetated areas under the boardwalk near ER1 (a, b) at two locations which were 2 cm away from each other (Aug. 8, 2006).

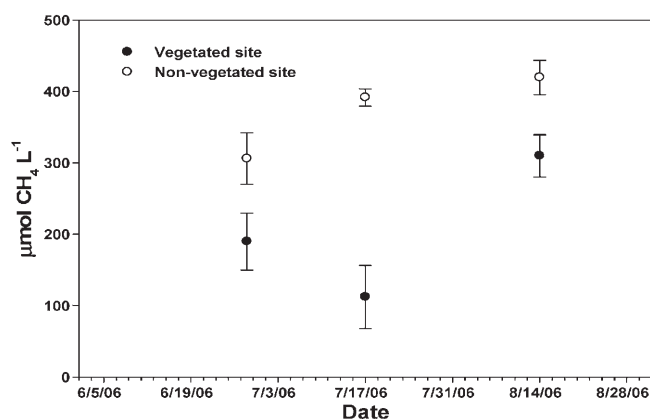
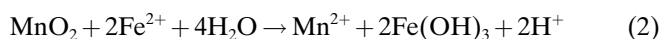
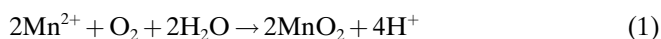


Fig. 5. Porewater CH<sub>4</sub> concentrations at vegetated site and nonvegetated site.

microelectrodes have the power to determine multiple redox species in situ at (sub)millimeter scale to examine the geochemistry of heterogeneous environments in soil.

As Mn(II) overlaps with O<sub>2</sub> in all vegetated areas studied, Mn(II) can oxidize to Mn(III, IV) solid phases (Eq. 1) which in turn also can oxidize Fe(II) to supply Fe(III) (Eq. 2) for bacterial Fe(III) reduction.



These reactions along with trace and nondetectable amounts of O<sub>2</sub> passing along plant roots are a way of transferring oxidation capacity deeper into the sediments.

In Figure 3a, the reaction of Mn(II) with O<sub>2</sub> is not complete as the gradient of O<sub>2</sub> decay in the surface is 109.5 µM/mm and for Mn(II) decay to the surface is only 80 µM/mm. Thus O<sub>2</sub> is in excess but does not quantitatively oxidize Mn(II) as some Mn(II) escapes to the overlying water. Much of the O<sub>2</sub> is likely used in organic matter decomposition. Likewise the Mn(II) gradient that overlaps with Fe(II) at ca. 5 mm is 38.2 µM/mm whereas the Fe(II) gradient is 367 µM/mm. These data indicate that much of the dissolved Fe(II) is produced from the reduction of Fe(III) solid phases by bacteria during the decomposition of organic matter [20, 28]. The Fe redox cycle can be represented schematically in Figure 6. Apparently there is not enough solid phase MnO<sub>2</sub> to react with the Fe(II) generated, thus Fe(II) reaches higher concentrations (mM) relative to Mn(II) in sediments.

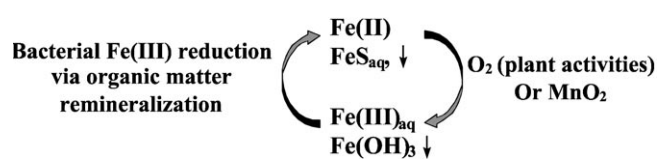


Fig. 6. Schematic describing the redox chemistry of iron in the sediments at Jug Bay.

At site ER2, Mn(II) was dominant after O<sub>2</sub> was consumed (Fig. 3b, 3c). At both locations, Mn(II) was detected down to 8 cm. Fe was not detected. A similar pattern was found at ER3 (Fig. 3d) where Mn(II) also dominated until Fe(II) dramatically increased at about 10 cm. The diagenetic redox sequence spanning to deeper depths at ER2 and ER3 than at ER1 is probably due to (1) more organic matter decomposition by manganese oxides at ER2 and ER3 (different plants at each site) and (2) sediments being more inundated by tidal influence as ER2 and ER3 are closer to the river.

At nonvegetated areas (Fig. 4a, 4b), O<sub>2</sub> was undetectable. Mn(II), Fe(II) and soluble Fe(III) were measured at the surface of the sediments and the vertical profiles are less variable than those at vegetated areas. Thus Fe/Mn cycling as shown in Figure 6 does not occur. FeS<sub>aq</sub> was measured below 1.5 mm, much shallower than at vegetated areas at ER3 (Fig. 3d, below 9.7 cm), which also indicates that roots transfer oxidation capacity deeper into the vegetated soil.

In situ electrochemical measurements demonstrate that Mn(III, IV) and Fe(III) reduction was the dominant pathway in anaerobic carbon metabolism in Jug Bay wetlands during summer. Plants introduce O<sub>2</sub> through roots which make the rhizosphere enhance biotic and abiotic cycling of Mn and Fe. Plants also can produce organic chelators and release them to soil porewaters to maintain Fe(III) in a soluble form for bacteria Fe(III) reduction [18, 29]. The abundances of Fe(II)-oxidizing bacteria (FeOB) and Fe(II)-reducing bacteria (FeRB) are normally much higher in the rhizosphere than in nonrhizosphere soils [30]. Mn biogeochemical cycling may also play a similar role as Fe in anaerobic carbon metabolism in wetlands. This has not been explored in detail in previous work. Plant-driven Fe(Mn) cycling helps suppress methane production, which has global warming implications [21].

O<sub>2</sub> availability in the rhizosphere can vary diurnally and seasonally due to plant driven processes. Our ongoing research will document the spatial and temporal chemical changes in wetlands to better understand biogeochemical processes in wetlands.

#### 4. Conclusion

The solid-state Au/Hg voltammetric microelectrode indicated significant Fe and Mn redox speciation in situ in wetland soils. The electrochemical measurements demonstrate that Mn(III, IV) and Fe(III) reduction were the dominant pathways in anaerobic carbon metabolism in Jug Bay wetlands during summer, which is also supported by porewater CH<sub>4</sub> measurements. Porewater methane measurements indicated that methane concentrations are lower in vegetated soils than in nonvegetated soils. Thus electrochemical determination of Fe and Mn may be useful as a proxy for understanding methanogenesis as plant-driven Fe(Mn) cycling suppressed methane production.

## 5. Acknowledgement

This project was supported by a grant from the National Science Foundation (DEB-0516121).

## 6. References

- [1] P. J. Brendel, G. W. Luther III, *Environ. Sci. Technol.* **1995**, *29*, 751.
- [2] G. W. Luther III, B. T. Glazer, S. Ma, R. E. Trouwborst, T. S. Moore, E. Metzger, C. Kraiya, T. J. Waite, G. Druschel, B. Sundby, M. Taillefert, D. B. Nuzzio, T. M. Shank, B. L. Lewis, P. J. Brendel, *Mar. Chem.* **2007**, doi:10.1016/j.marchem.2007.03.002.
- [3] G. W. Luther III, B. Glazer, S. Ma, R. Trouwborst, B. R. Shultz, G. Druschel, C. Kraiya, *Aquat. Geochem.* **2003**, *9*, 87.
- [4] G. W. Luther III, C. E. Reimers, D. B. Nuzzio, D. Lovalvo, *Environ. Sci. Technol.* **1999**, *33*, 4352.
- [5] G. W. Luther III, B. T. Glazer, L. Hohman, J. I. Popp, M. Taillefert, T. F. Rozan, P. J. Brendel, S. M. Theberge, D. B. Nuzzio, *J. Environ. Monit.* **2001**, *3*, 61.
- [6] G. W. Luther III, T. F. Rozan, M. Taillefert, D. B. Nuzzio, C. Di Meo, T. M. Shank, R. A. Lutz, S. C. Cary, *Nature* **2001**, *410*, 813.
- [7] G. W. Luther III, A. Bono, M. Taillefert, S. C. Cary, *Environmental Electrochemistry: Analyses of Trace Element Biogeochemistry* (Ed: M. Taillefert, T. Rozan) ACS Symposium Series, American Chemical Society, Washington, DC **2002**, p. 54.
- [8] G. W. Luther III, S. Ma, R. Trouwborst, B. Glazer, M. Blickley, R. W. Scarborough, M. G. Mensinger, *Estuaries* **2004**, *27*, 551.
- [9] C. Chapman, C. G. Van Den Berg, *Environ. Sci. Technol.* **2005**, *39*, 2769.
- [10] B. Sundby, M. Caetano, C. Vale, C. Gobeil, G. W. Luther III, D. B. Nuzzio, *Environ. Sci. Technol.* **2005**, *39*, 2080.
- [11] S. Ma, E. B. Whereat, G. W. Luther III, *Aquat. Microb. Ecol.* **2006**, *44*, 279.
- [12] W. J. Cai, P. Zhao, Y. Wang, S. M. Theberge, A. Witter, G. W. Luther III, *Environmental Electrochemistry: Analyses of Trace Element Biogeochemistry* (Ed: M. Taillefert, T. Rozan) ACS Symposium Series, American Chemical Society, Washington, DC **2002**, p. 188.
- [13] M. Taillefert, S. Neuhuber, G. Bristow, *Geochem. Trans.* **2007**, *8*: 6 doi:10.1186/1467-4866-8-6.
- [14] M.-L. Tercier-Waeber, C. Belmont-Hebert, J. Buffle, *Environ. Sci. Technol.* **1998**, *32*, 1515.
- [15] M.-L. Tercier-Waeber, J. Buffle, F. Confalonieri, G. Riccardi, A. Sina, F. Graziottin, G. C. Fiaccabrino, M. Koudelka-Hep, *Measure. Sci. Technol.* **1999**, *10*, 1202.
- [16] P. N. Froelich, G. P. Klinkhammer, M. L. Bender, N. A. Luedtke, G. R. Heath, D. Cullen, P. Dauphin, D. Hammond, B. Hartman, V. Maynard, *Geochim. Cosmochim. Acta* **1979**, *43*, 1075.
- [17] W. S. Reebergh, *Chem. Rev.* **2007**, *107*, 486.
- [18] J. E. Kostka, G. W. Luther III, *Biogeochemistry* **1995**, *29*, 159.
- [19] J. E. Kostka, B. Gribsholt, E. Petrie, D. Dalton, H. Skelton, E. Kristensen, *Limnol. Oceanogr.* **2002**, *47*, 230.
- [20] E. E. Roden, R. G. Wetzel, *Limnol. Oceanogr.* **1996**, *41*, 1733.
- [21] S. C. Neubauer, K. Givler, S. K. Valentine, J. P. Megonigal, *Ecology* **2005**, *86*, 3334.
- [22] J. V. Weiss, D. Emerson, J. P. Megonigal, *FEMS Microbiology Ecol.* **2004**, *48*, 89.
- [23] D. J. Wuebbles, K. Hayhoe, *Earth Sci. Rev.* **2002**, *57*, 177.
- [24] A. S. Marsh, D. P. Rasse, B. G. Drake, J. P. Megonigal, *Estuaries* **2005**, *28*, 694.
- [25] G. W. Luther III, B. Sundby, B. L. Lewis, P. J. Brendel, N. Silverberg, *Geochim. Cosmochim. Acta* **1997**, *61*, 4043.
- [26] M. Taillefert, A. B. Bono, G. W. Luther III, *Environ. Sci. Technol.* **2000**, *34*, 2169.
- [27] D. Rickard, G. W. Luther, *Chem. Rev.* **2007**, *107*(2), 514.
- [28] D. Emerson, J. V. Weiss, *Geomicrobiol. J.* **2004**, *21*, 405.
- [29] G. W. Luther, III, J. E. Kostka, T. M. Church, B. Sulzberger, W. Stumm, *Mar. Chem.* **1992**, *40*, 81.
- [30] J. V. Weiss, D. Emerson, S. M. Backer, J. P. Megonigal, *Biogeochemistry* **2003**, *64*, 77.